

Collective dynamics in liquid lead: Generalized propagating excitations

Taras Bryk* and Ihor Mryglod

Institute for Condensed Matter Physics, National Academy of Sciences of Ukraine, 1 Svientsitskii Street, UA-79011 Lviv, Ukraine

(Received 20 October 2000; published 10 April 2001)

A microscopic approach to the investigation of generalized collective excitations, developed recently for pure liquids, is applied to the study of the spectrum of collective excitations in a liquid metal. The calculations are performed for liquid lead at two temperatures (above the melting point and in high-temperature region) and the results are compared. From the analysis of spectra, obtained for different basis sets of dynamical variables, we conclude that there exist three branches of propagating collective excitations, which correspond to sound and heat (high- and low-frequency) waves in the liquid. It is shown that the branch of low-frequency heat waves contains a propagation gap in the hydrodynamic region. An analytical expression for the width of the propagation gap for low-frequency heat waves is derived.

DOI: 10.1103/PhysRevE.63.051202

PACS number(s): 61.20.Ja, 61.20.Lc, 05.20.Jj

I. INTRODUCTION

Liquid metals are known as the systems with well-defined collective propagating excitations, which could be visible as the side peaks in the dynamical structure factor $S(k, \omega)$ up to $k \sim 1 \text{ \AA}^{-1}$ or even more [1], k and ω being a wave number and frequency, respectively. Although the shape of $S(k, \omega)$ contains in general the information about all the processes in a liquid with long- and short-time scales, the side peaks are usually considered as attributed mainly to the propagating density waves, so that it is believed that the dispersion of sound excitations can be extracted from the positions of Brillouin peaks. Well beyond the hydrodynamic region the propagating excitations become overdamped and can be observed in the dynamic structure factor as the more or less pronounced shoulder, which have been visible in liquid bismuth [2], for instance, even on the high- k side of the main peak of the static structure factor $S(k)$. Recently, analysis of scattering experiments and molecular dynamics (MD) simulations, performed for a semimetallic liquid Ga, has led to a conclusion about the existence of an additional “nonacoustic” high-frequency branch in the spectrum of collective excitations [3].

Up to now the dynamics of binary systems had just been considered from the point of view of the existence of several branches of propagating excitations. The high-frequency excitations in binary liquids were associated with the “fast-sound” phenomenon [4–6] or with opticlike excitations in the case of ionic solutions [7,8]. In the most recent investigations [9,10] it was shown that opticlike excitations, caused by mass-concentration fluctuations, exist also in mixtures of simple liquids. However, we have found only a few reports focused on the possibility to observe the nonhydrodynamic excitations in simple liquids. For example, in Ref. [11] the analysis of thermal neutron-scattering experiments for liquid Cs and Rb near the melting point allowed one to conclude that in these metals short-wavelength collective excitations with anomalous dispersion could be observed for wave num-

bers beyond the hydrodynamic region. These propagating modes were identified as “zero-sound” modes with the damping coefficient, varying linearly with wave number. However, neither in [11] nor in [3] has the origin of nonacoustic collective excitations been clearly established.

As another example of nonhydrodynamic collective excitations one can take the heat waves, which are sometimes called the “second-sound” modes or thermal waves. Heat waves in liquids are propagating collective excitations, introduced for the explanation of some experiments on heat transfer [12]. Within standard hydrodynamics only two mechanisms of heat transfer in a liquid can be considered: thermodiffusion and propagating sound waves. Since propagating heat waves cannot be obtained within a hydrodynamic treatment, they belong to so-called *kinetic* collective excitations, possessing a finite lifetime even in the hydrodynamic limit, and contribute mainly to the relevant time correlation functions beyond the hydrodynamic region. The dispersion of these collective excitations is not known *a priori* and cannot be studied within standard hydrodynamic theory or within the phenomenological approach, based on a telegraphlike equation [12]. Therefore, a microscopic study of this problem would also be of great interest.

It is worth mentioning that the method, widely used in the literature for the estimation of the dispersion of propagating collective excitations from the maximum position of the relevant spectral function, can be only applied under some special conditions (e.g., well-defined and well-separated collective excitations) and fails beyond the hydrodynamic region. For large wave numbers the propagating modes usually become overdamped and are mixed each with the other [13], so that any time correlation function contains in general contributions from all collective excitations (extended hydrodynamic and kinetic ones). Therefore, a theoretical method for the analysis of time correlation functions which allows us to separate the corresponding mode contributions and to study self-consistently the kinetic propagating excitations is needed.

In the hydrodynamic limit ($k \rightarrow 0$, $\omega \rightarrow 0$) the collective-mode spectrum can be studied analytically [14,15]. For small wave numbers the longitudinal dynamics of a pure liquid is well described within the three-variable set of hydrodynamic

*Present address: Department of Chemistry, University of Houston, Houston, TX 77004.

variables [the particles' density $n(k,t)$, the density of longitudinal current $J_l(k,t)$, and the energy density $e(k,t)$], connected with the densities of additive conserved quantities. By solving the hydrodynamic equations, the spectrum of three hydrodynamic modes (two propagating sound excitations and the relaxing thermodiffusive mode), associated with the slowest dynamical processes in the system, can be found. Beyond the hydrodynamic region short-time kinetic processes become more important and standard hydrodynamics fails to explain the dynamic properties of dense fluids for intermediate and large values of k and ω . There were several attempts (see, e.g., [16,17]) to modify the analytical expressions, found within the hydrodynamic theory for the hydrodynamic time correlation functions or their spectral functions, in which the idea of extended k -dependent hydrodynamic modes has been used. However, it is evident that such approaches cannot be used for the study of nonhydrodynamic kinetic excitations which are in fact additional modes excluded from the hydrodynamic treatment.

A concept of generalized collective modes (GCM's), proposed initially in [17,18] for the investigation of time correlation functions of liquids beyond the hydrodynamic region and developed later [19,13] in a computer-adapted form being free of any adjustable parameters, is now one of the most powerful methods for the study of extended k -dependent collective modes, which allows us to consider simultaneously the hydrodynamic and kinetic processes. The main idea of this method is to extend the basis set of dynamical variables by including in addition to hydrodynamic variables also their time derivatives, which, it is supposed, describe correctly the short-time processes. For practical needs the problem of liquid dynamics can be reduced [20] to the spectral problem for the so-called generalized hydrodynamic matrix. The eigenvalues of the generalized hydrodynamic matrix give the spectrum of extended collective modes and the mode contributions to time correlation functions are expressed via the associated eigenvectors. The static correlation functions as well as so-called "hydrodynamic" correlation times can be directly obtained in computer experiments or evaluated by means of the equilibrium theory. In general, the basis set of N_v dynamical variables generates the $N_v \times N_v$ secular equation and results in N_v generalized collective modes (eigenvalues). Any time correlation function, constructed on the dynamic variables from the basis set and calculated within the GCM approach (such a function will be called a GCM function), can be represented as a sum of the N_v -mode contributions. In numerous studies, performed for Lennard-Jones liquids [18,19], liquid metallic Cs [21,22] and semimetallic Bi [23], and liquid water [24], it has been proved that the GCM method is very useful for the investigation of time correlation functions and the spectra of collective excitations in pure liquids. Moreover, the same conclusion follows also from the results obtained for binary liquids [25]: in particular, for Lennard-Jones mixtures [26], "fast-sound" mixture $\text{He}_{65}\text{Ne}_{35}$ [27,28], liquid glass-forming metallic alloy $\text{Mg}_{70}\text{Zn}_{30}$ [29,10], and metallic molten alloy Li_4Pb [10]. Hence, this method was tested in many applications and can be used as an appropriate one to attack the problem of the observed kinetic excitations in a simple liquid.

Among the N_v eigenvalues of the generalized hydrodynamic matrix, the lowest-lying ones (in the small- k region) correspond usually to the generalized hydrodynamic modes. The number of such modes depends on the number of hydrodynamic variables (three longitudinal modes in the case of a pure liquid and four ones for a binary mixture), and their properties in the hydrodynamic limit are in complete agreement with the predictions of linear hydrodynamics. All the other eigenvalues correspond to the *kinetic* modes, being responsible for the short-time behavior. We note once again that these modes cannot be obtained within the standard hydrodynamic treatment, and their contributions can be very significant beyond the hydrodynamic region. In particular, it was clearly shown for binary liquids that the "fast-sound" phenomenon [28] and the appearance of opticlike excitations in many-component liquids [9,10] could be explained only by taking into account kineticlike processes. In the case of simple liquids even the physical origin of the kinetic-mode formation was not studied in detail. In this paper we consider this problem in more detail, taking as an example the dynamical properties of liquid lead.

The goals of this study are (i) to obtain the spectra of generalized collective excitations for liquid lead at different temperatures, (ii) to study the origin of mode formation for all the branches of longitudinal collective modes obtained, (iii) to focus attention on the behavior of heat fluctuations in a liquid metal and the emergence of heat waves, and (iv) to discuss in comparison the results obtained for generalized collective modes at high and low (above the melting point) temperatures. In our study we use the many-variable approximations of the generalized collective mode approach in parameter-free form [30], developed recently for simple liquids (see, e.g., [20]).

The paper is organized as follows: in Sec. II a brief outline of the method, used for calculations of collective excitation spectra, is given; the results, obtained the generalized collective modes, are analyzed in Sec. III, and the conclusions are formulated in Sec. IV. We will report the results obtained for the separated mode contributions of liquid lead in Ref. [41].

II. GCM APPROACH: NINE-VARIABLE APPROXIMATION

Let us consider a spatially homogeneous, isotropic system of N identical classical particles of mass m in the volume V . We start from the definition of the square matrix of time correlation functions $\mathbf{F}^0(k,t)$, each element of which is defined as follows:

$$\mathbf{F}_{ij}^0(k,t) = \langle A_i(\mathbf{k},0) A_j^*(\mathbf{k},t) \rangle, \quad (1)$$

where the dynamic variables $A_i(\mathbf{k},t)$ and $A_j(\mathbf{k},t)$ belong to the basis set $\{A_i(k,t)\}$. The basis set $\{A_i(k,t)\}$ includes all the densities of conserved quantities as well as their time derivatives. Let us suppose that the N_v microscopic dynamic variables $A_i(\mathbf{k},t)$ form the basis set $\{A_i(k,t)\}$, so that $\mathbf{F}^0(k,t)$ is an $N_v \times N_v$ square matrix.

The matrix equation for the Laplace transform $\tilde{\mathbf{F}}^0(k, z)$ of $\mathbf{F}^0(k, t)$ can be written in the well-known form (see, e.g., [15])

$$[z\mathbf{I} - i\mathbf{\Omega}(k) + \tilde{\mathbf{M}}(k, z)]\tilde{\mathbf{F}}^0(k, z) = \mathbf{F}^0(k, 0), \quad (2)$$

where $i\mathbf{\Omega}(k)$ and $\tilde{\mathbf{M}}(k, z)$ are the frequency matrix and the matrix of the memory functions, respectively. In the Markovian approximation for the memory functions, when $\tilde{\mathbf{M}}(k, z) \approx \tilde{\mathbf{M}}(k, 0)$, one obtains

$$[z\mathbf{I} + \mathbf{T}(k)]\tilde{\mathbf{F}}^M(k, z) = \mathbf{F}^0(k, t=0), \quad (3)$$

where

$$\mathbf{T}(k) = -i\mathbf{\Omega}(k) + \tilde{\mathbf{M}}(k, 0) = \mathbf{F}^0(k, 0)[\tilde{\mathbf{F}}^0(k, 0)]^{-1} \quad (4)$$

is the so-called generalized hydrodynamic matrix, $\tilde{\mathbf{F}}^M$ denotes the Laplace-transformed matrix of time correlation functions to be found in the Markovian approximation, and \mathbf{I} is the identity matrix. Using Eq. (3) it is straightforward to derive the following equalities:

$$\int_0^\infty \mathbf{F}^M(k, t) dt = \int_0^\infty \mathbf{F}^0(k, t) dt, \quad (5)$$

$$\mathbf{F}^M(k, t=0) = \mathbf{F}^0(k, t=0), \quad (6)$$

which are important from the point of view of sum rules [31,32] and connect the moments of time correlation functions $\mathbf{F}^M(k, t)$ and $\mathbf{F}^0(k, t)$.

The matrix equation (3) can be solved analytically in terms of eigenvalues $z_\alpha(k)$ and eigenvectors $\hat{X}_\alpha = \{X_{i,\alpha}\}$ of the matrix $\mathbf{T}(k) = \|T_{ij}(k)\|$ [see Eq. (4)],

$$\sum_{j=1}^{N_v} T_{ij}(k) X_{j,\alpha} = z_\alpha(k) X_{i,\alpha}, \quad i=1, \dots, N_v, \quad (7)$$

so that we obtain

$$\tilde{\mathbf{F}}_{ij}^M(k, z) = \sum_{\alpha=1}^{N_v} \frac{G_{ij}^\alpha(k)}{z + z_\alpha(k)}, \quad (8)$$

where

$$G_{ij}^\alpha(k) = \sum_{l=1}^{N_v} X_{i\alpha} X_{\alpha l}^{-1} F_{lj}(k, 0) \quad (9)$$

is the weight coefficient describing a contribution of the mode z_α to the function $\tilde{\mathbf{F}}_{ij}^M(k, z)$. In time representation one has the form

$$F_{ij}^M(k, t) = \sum_{\alpha=1}^{N_v} G_{ij}^\alpha(k) \exp\{-z_\alpha(k)t\}. \quad (10)$$

Hence, as is seen from Eq. (10), the time correlation function $F_{ij}^M(k, t)$ can be expressed within the generalized mode approach as a weighted sum of N_v exponential terms, and each term of this sum is associated with the relevant effective collective mode $z_\alpha(k)$. The precision of the GCM function (10) in the N_v -mode description is controlled by the equalities (5) and (6).

Within the nine-variable approximation [13] of the parameter-free GCM method the basis set of dynamical variables for the case of longitudinal dynamics in pure liquids consists of the following operators:

$$\mathbf{A}^{(9)}(k, t) = \{n(k, t), J_l(k, t), e(k, t), \dot{J}_l(k, t), \dot{e}(k, t), \ddot{J}_l(k, t), \ddot{e}(k, t), \dddot{J}_l(k, t), \dddot{e}(k, t)\}, \quad (11)$$

where overdots denote the order of the time derivative of the relevant operator. The basis set of dynamical variables is applied to generate the eigenvalue problem from the generalized Langevin equation in Markovian approximation [19,13]. In our case the 9×9 Hermitian matrix of static correlation functions $\mathbf{F}^0(k, t=0)$ has the following form:

$$\mathbf{F}^0(k) = \begin{pmatrix} f_{nn} & 0 & f_{ne} & -ikf_{JJ} & 0 & 0 & -kf_{je} & ikf_{jj} & 0 \\ 0 & f_{JJ} & 0 & 0 & -if_{je} & -f_{jj} & 0 & 0 & if_{j\dot{e}} \\ f_{ne} & 0 & f_{ee} & -if_{j\dot{e}} & 0 & 0 & -f_{e\dot{e}} & if_{j\ddot{e}} & 0 \\ ikf_{JJ} & 0 & if_{j\dot{e}} & f_{jj} & 0 & 0 & -if_{j\ddot{e}} & -f_{j\ddot{j}} & 0 \\ 0 & if_{j\dot{e}} & 0 & 0 & f_{e\ddot{e}} & -if_{j\ddot{e}} & 0 & 0 & -f_{e\ddot{e}} \\ 0 & f_{jj} & 0 & 0 & if_{j\ddot{e}} & f_{j\ddot{j}} & 0 & 0 & -if_{j\ddot{e}} \\ -kf_{je} & 0 & -f_{e\dot{e}} & if_{j\dot{e}} & 0 & 0 & f_{e\ddot{e}} & -if_{j\ddot{e}} & 0 \\ -ikf_{jj} & 0 & -if_{j\dot{e}} & -f_{j\ddot{j}} & 0 & 0 & if_{j\ddot{e}} & f_{j\ddot{j}} & 0 \\ 0 & -if_{j\dot{e}} & 0 & 0 & -f_{e\ddot{e}} & if_{j\ddot{e}} & 0 & 0 & f_{e\ddot{e}} \end{pmatrix}, \quad (12)$$

where for simplicity $f_{ij}(k)$ are shown as the absolute values of relevant static correlation functions.

Similarly, taking into account the properties of time correlation functions [18,19], one gets for the matrix $\tilde{\mathbf{F}}^0(k) = \tilde{\mathbf{F}}^0(k, z=0)$

$$\tilde{\mathbf{F}}^0(k) = \begin{pmatrix} \tau_{nn}f_{nn} & \frac{i}{k}f_{nn} & \tau_{ne}f_{ne} & 0 & f_{ne} & -ikf_{JJ} & 0 & 0 & -kf_{je} \\ \frac{i}{k}f_{nn} & 0 & \frac{i}{k}f_{ne} & f_{JJ} & 0 & 0 & -if_{je} & -f_{jj} & 0 \\ \tau_{nn}f_{ne} & \frac{i}{k}f_{ne} & \tau_{ee}f_{ee} & 0 & f_{ee} & -if_{je} & 0 & 0 & -f_{\ddot{e}e} \\ 0 & -f_{JJ} & 0 & 0 & if_{je} & f_{jj} & 0 & 0 & -if_{\ddot{j}e} \\ -f_{ne} & 0 & -f_{ee} & if_{je} & 0 & 0 & f_{\ddot{e}e} & -if_{\ddot{j}e} & 0 \\ -ikf_{JJ} & 0 & -if_{je} & -f_{jj} & 0 & 0 & if_{\ddot{j}e} & f_{\ddot{j}j} & 0 \\ 0 & -if_{je} & 0 & 0 & -f_{\ddot{e}e} & if_{\ddot{j}e} & 0 & 0 & f_{\ddot{e}\ddot{e}} \\ 0 & f_{jj} & 0 & 0 & -if_{\ddot{j}e} & -f_{jj} & 0 & 0 & if_{\ddot{j}\ddot{e}} \\ kf_{je} & 0 & f_{\ddot{e}e} & -if_{\ddot{j}e} & 0 & 0 & -f_{\ddot{e}\ddot{e}} & if_{\ddot{j}\ddot{e}} & 0 \end{pmatrix}, \quad (13)$$

where

$$\tau_{ij}(k) = \frac{1}{F_{ij}^0(k, t=0)} \int_0^\infty F_{ij}^0(k, t) dt \quad (14)$$

are the ‘‘hydrodynamic’’ correlation times, which are the only quantities within the parameter-free GCM method that keep the information about time-dependent properties of the system.

It is seen in Eqs. (12) and (13) that in order to apply the developed method for the study of collective-mode spectrum of a particular liquid, one has to calculate the static correlation functions needed as well as the ‘‘hydrodynamic’’ correlation times $\tau_{ij}(k)$. In particular, this can be done by combining MD simulations with the analytical expressions derived.

III. RESULTS AND DISCUSSION

We performed MD simulations in a standard microcanonical ensemble for liquid Pb at two thermodynamic points: a high-temperature state at 1170 K with number density $n = 0.0289 \text{ \AA}^{-3}$ and a state above melting temperature at 623 K with number density $n = 0.03094 \text{ \AA}^{-3}$. In molecular dynamics we studied a system of 1000 particles interacting through oscillating potential $\Phi_{ij}(r)$ at constant volume $V = L^3$. The smallest wave numbers achieved in MD were $k_{\min}^h = 0.1928 \text{ \AA}^{-1}$ and $k_{\min}^l = 0.1973 \text{ \AA}^{-1}$ for high- and low-temperature states, respectively. The time evolution of hydrodynamic variables and their time derivatives was observed during a production run over 3×10^5 steps for each temperature. The effective two-body potential was taken in an analytical form from Ref. [33]. This potential reproduced very well the experimental static structure factor of liquid lead over a wide temperature range [33].

A. Static properties

Static structure factors $S(k)$ at two temperatures considered are shown in Fig. 1. The function $S(k)$, obtained as the Fourier transform of the pair correlation functions (shown by crosses), is in very good agreement with the static average $f_{nn}(k)$ (shown by boxes), evaluated directly by MD. This

means a good reliability (enough configurations for good statistics) of the static averages directly evaluated in MD. One can note that for both temperatures the static structure factors have the main peaks at $k_p \approx 2.3 \text{ \AA}^{-1}$. The amplitude of the main peak at the lower-temperature state is much higher than at the high-temperature state.

The static correlation functions $f_{ne}(k)$, $f_{ee}(k)$, and $f_{je}(k)$, evaluated directly in MD for high- and low-temperature states (circles and boxes, respectively), are shown in Fig. 2. Within Newtonian dynamics any operator from the basis set $\mathbf{A}^{(9)}(k, t)$ can be expressed in an analytical form via positions and velocities of particles and spatial derivatives of the interatomic potential (see [19]). Therefore, one can evaluate directly in MD any static average between basis variables within the same precision. Due to the analytical form of the interatomic potential, we avoided a numerical evaluation of the spatial derivatives of $\Phi_{ij}(r)$, which were needed in MD in order to obtain the time evolution of dynamical variables from the basis set (11). This resulted in a very smooth k dependence of static averages directly evaluated in MD. From Fig. 2 one can see that the static averages $f_{ne}(k)$ and $f_{ee}(k)$ behave like the static structure factor $S(k)$, while the function $f_{je}(k)$ increases linearly with k in the small- k region [$f_{je}(k) \sim k$]. Another possibility for the calculation of $f_{je}(k)$ is to find numerically the second-order

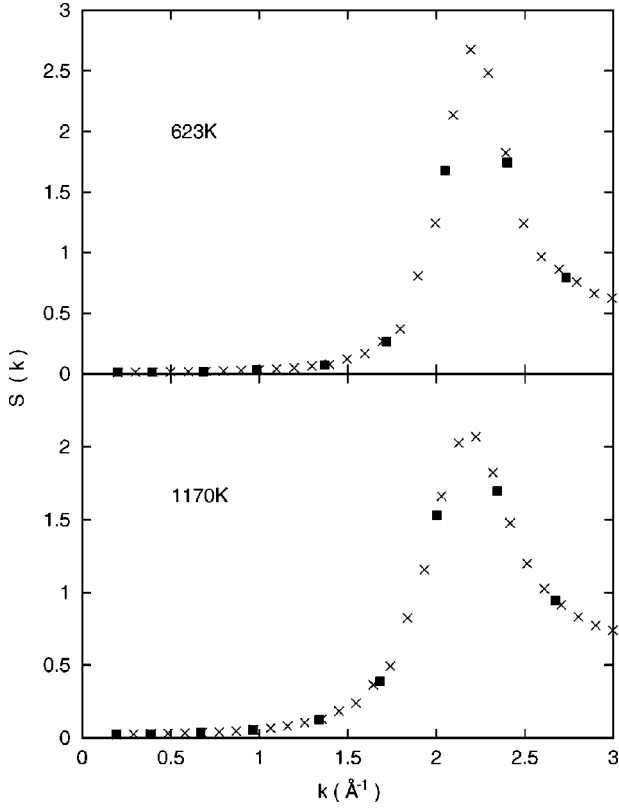


FIG. 1. Static structure factors for liquid Pb at two temperatures $T_l=623$ K and $T_h=1170$ K: Squares represent static averages $f_{nn}(k)$, evaluated directly in MD, and crosses correspond to $S(k)$, obtained via Fourier transform of the pair correlation function.

time derivative of the time correlation function $F_{ne}(k,t)$ at $t=0$. It is seen in Fig. 2 that both methods (the results of direct calculation of static averages are shown by open circles and open squares, and the dates for the numerical second derivative of the relevant time correlation functions are plotted by crosses) allow us to obtain almost identical values. In this study the numerical method for the evaluation of static averages (second one) was used only for calculations of the three highest-order static correlation functions, constructed on the operators with three dots. This allowed us to decrease sufficiently the time of MD production runs. All other static averages were directly obtained in MD simulations.

Using our MD results for the static correlation functions, shown in Figs. 1 and 2, we have obtained as well the k -dependent generalized thermodynamic quantities, defined by the expressions given in [18,19], namely,

$$H(k) = \frac{1}{k_B T k} f_{je}(k), \quad (15)$$

$$C_V(k) = \frac{1}{k_B T^2} \left[f_{ee}(k) - \frac{f_{ne}^2(k)}{f_{nn}(k)} \right], \quad (16)$$

$$\alpha(k)T = \frac{1}{k_B T} [H(k)f_{nn}(k) - f_{ne}(k)], \quad (17)$$

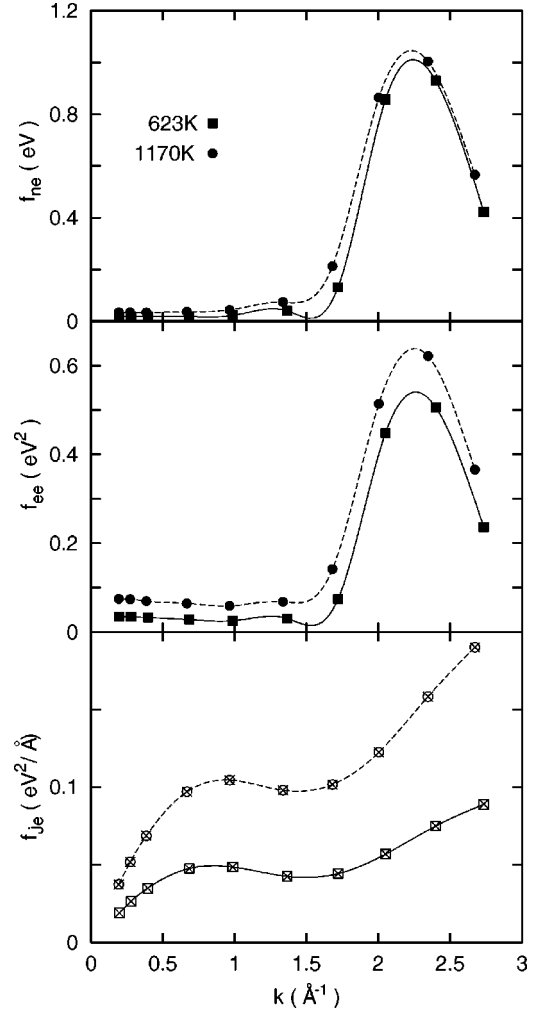


FIG. 2. Static averages $f_{ne}(k)$, $f_{ee}(k)$, and $f_{je}(k)$, evaluated directly in MD. Squares correspond to the low-temperature state at 623 K, and circles to the temperature 1170 K. In the lower frame crosses correspond to the values of $f_{je}(k)$, obtained via numerical derivatives of the relevant time correlation function at $t=0$. Lines denote the spline interpolation.

$$\gamma(k) = \frac{C_P(k)}{C_V(k)}, \quad C_P(k) = C_V(k) + \frac{k_B T^2 \alpha^2(k)}{f_{nn}(k)}, \quad (18)$$

where k_B denotes the Boltzmann constant, $H(k)$ is the generalized enthalpy per particle, $\alpha(k)$ is the generalized thermal expansion coefficient, and $C_V(k)$ and $C_P(k)$ are the generalized specific heats at constant volume and constant pressure per particle, respectively. In Figs. 3(a) and 3(b) the k dependence of these quantities is shown. The results obtained for liquid Pb can be compared with those found previously for the generalized thermodynamic quantities of Lennard-Jones fluid [19], liquid metallic Cs [21], and semi-metallic Bi [23]. The generalized enthalpy for Pb does not change sign as a function of k as was observed in the case of LJ liquid or Cs above the melting point, but such behavior is very similar to the case of liquid Bi. Perhaps, this is connected with the similarity in two-body potentials for Bi and Pb (see [2]). Another interesting feature is seen in the behav-

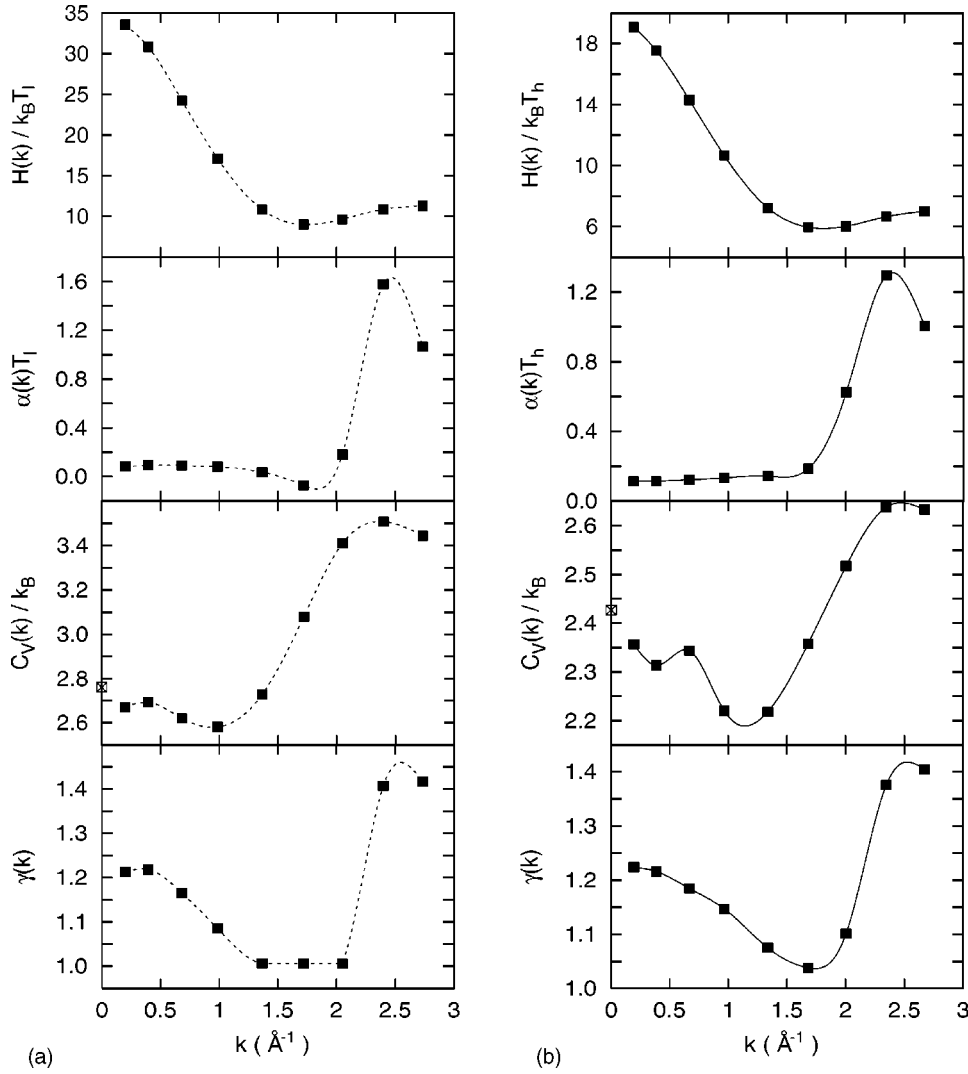


FIG. 3. Generalized thermodynamic quantities for liquid Pb at $T_l=623$ K (a) and $T_h=1170$ K (b): the generalized enthalpy per particle $H(k)$, the generalized thermal expansion coefficient $\alpha(k)$, the generalized specific heat at constant volume per particle $C_V(k)$, and the generalized ratio of specific heats $\gamma(k)$. The open square with a cross at $k=0$ for $C_V(k)$ denotes values estimated from temperature fluctuations in MD. Dotted and solid lines denote the spline interpolation.

ior of the generalized linear expansion coefficient $\alpha(k)$. In the range $k \sim 1.5-2.0 \text{ \AA}^{-1}$ this function for the low-temperature state at 623 K becomes negative, while at the higher temperature $\alpha(k)$ is always positive. For both temperatures the generalized linear expansion coefficient as a function of k has a maximum at the main peak position of the static structure factor. The existence of a negative peak on $\alpha(k)$ was also observed in a liquid Bi [23]. Such a specific feature requires additional study and the results will be reported elsewhere. The generalized specific heat $C_V(k)$ at constant volume has a maximum in the region of the main peak of static structure factor $k \approx k_p$. The open squares at $k=0$ show the values of C_V estimated from temperature fluctuations during an MD run. The generalized ratio of specific heats $\gamma(k)$ for the lower temperature [the lowest frame in Fig. 3(a)] has a wide minimum in the region $1.3-2.1 \text{ \AA}^{-1}$ with a value of ~ 1.0 , which indicates the region of applicability of viscoelastic theory for liquid Pb above the melting point. This is in contrast with the result found for higher temperature where the generalized ratio of specific heats $\gamma(k)$ takes the lowest value ~ 1.04 at $k \sim 1.6 \text{ \AA}^{-1}$, and the minimum is more sharp. This means that at higher temperatures the coupling between thermal and density fluctuations

becomes much stronger, so that the range of application of the viscoelastic approximation decreases.

B. Time correlation functions

The normalized MD-derived density-density, density-energy, and energy-energy time correlation functions are shown in Figs. 4(a) and 4(b) for two wave numbers at the low- and high-temperature states, respectively. For small wave numbers all these functions display strong oscillations with almost the same period. In contrast to liquid Cs [21,34], where oscillations of energy-energy time correlation functions are overdamped even for small k values, in the case of liquid Pb the energy-energy and energy-density time correlation functions have even more pronounced oscillations than the density-density time correlation functions. Such a behavior is observed in the k region up to $\sim 1 \text{ \AA}^{-1}$. It is interesting that at two temperatures and very close k values, considered in MD, the difference in amplitude of oscillations is clearly seen in the time-dependence of time correlation functions, especially for the density-energy and energy-energy time correlation functions.

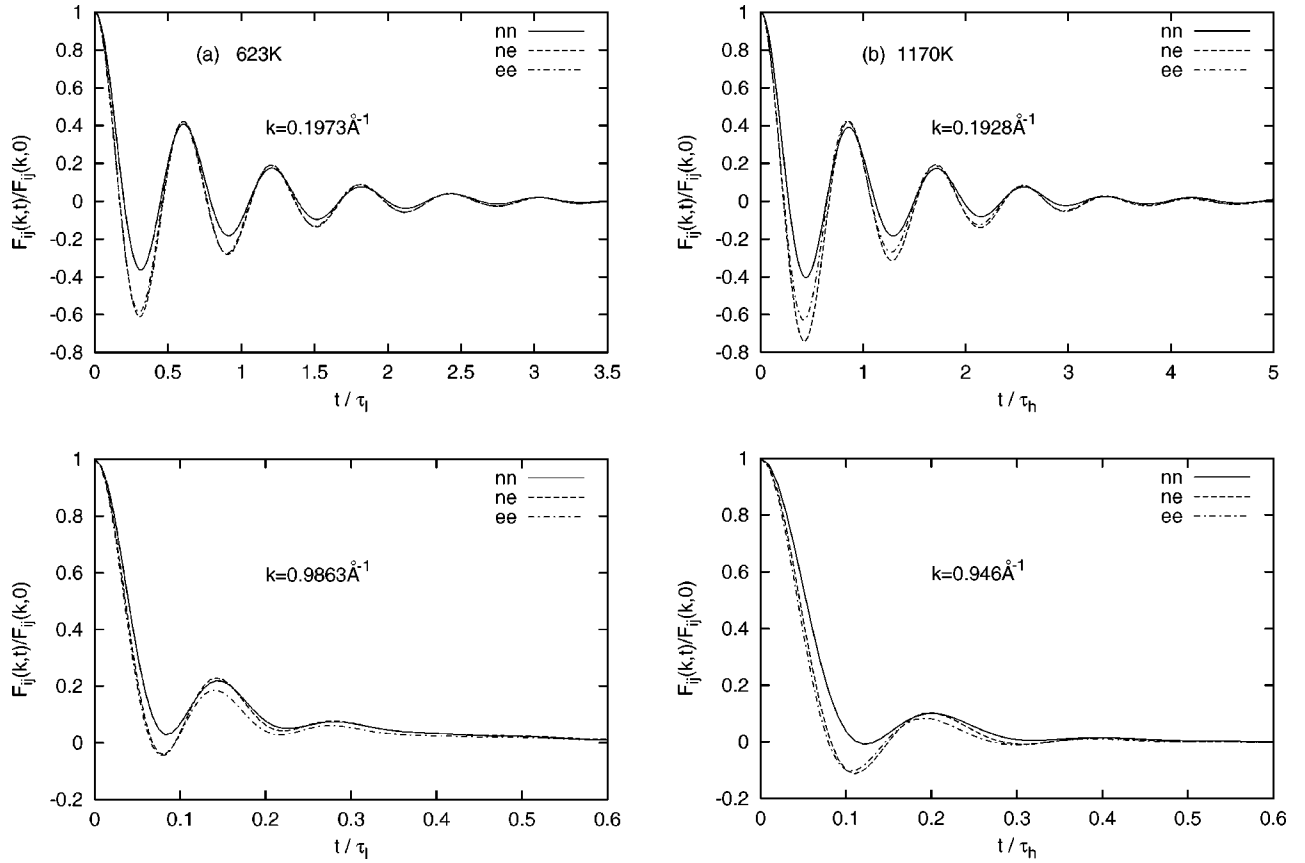


FIG. 4. Normalized time correlation functions for two k values: $F_{nn}(k,t)$ (solid line), and $F_{ne}(k,t)$ (dashed line), $F_{ee}(k,t)$ (dashed-dotted line) at $T_l = 623$ K (a) and $T_h = 1170$ K (b). Time scales are $\tau_l = 3.2064$ ps and $\tau_h = 2.3935$ ps, respectively.

For the case of a simple liquid there exist three ‘‘hydrodynamic’’ correlation times, which are in fact the input parameters of the GCM method and contain information about the time-dependent properties of the system investigated. In Fig. 5 the correlation times $\tau_{nn}(k)$, $\tau_{ne}(k)$, and $\tau_{ee}(k)$ (multiplied by k^2) are shown. One can see that all these functions are very similar and reflect the behavior of structure factor $S(k)$ within the entire k range studied. In the hydrodynamic limit $k \rightarrow 0$ the correlation times are inverse proportional to k^2 , so that the functions $k^2\tau_{ij}(k)$ tend to finite nonzero values when $k \rightarrow 0$. The similar behavior of all three correlation times as functions of wave number can be understood from Fig. 4, where the relevant time correlation functions are shown.

C. Spectrum of generalized collective modes

The eigenvalues of the generalized hydrodynamic matrix $\mathbf{T}(k)$, defined by Eq. (4) and generated by the basis set (11), were calculated for liquid Pb at the low- and high-temperature states. The results are shown in Figs. 6(a) and 6(b), respectively. As the functions of k these eigenvalues form the spectra of generalized collective excitations. It is seen in Fig. 6 that for both temperatures the spectra contain in general four branches of generalized propagating modes: three of them exist over the whole k range considered, and one branch, denoted as $z_1(k)$, has the propagating gap in the small- k region and appears for k larger than some

temperature-dependent value. Propagating modes are associated with the complex-conjugated eigenvalues

$$z_{\alpha}^{\pm}(k) = \sigma_{\alpha}(k) \pm i\omega_{\alpha}(k), \quad \alpha = 1, \dots, 4,$$

where $\omega_{\alpha}(k)$ and $\sigma_{\alpha}(k)$ are the frequency and damping of the relevant collective excitation, respectively. The imaginary and real parts of the complex-conjugated eigenvalues are shown in Figs. 6(a) and 6(b) by the same symbols connected by spline-interpolated solid lines. Three purely real eigenvalues, marked for convenience as $d_{\alpha}(k)$ with $\alpha = 1, 2, 3$, are shown in the lower frames of Figs. 6(a) and 6(b) by symbols connected by spline-interpolated dotted lines. One can see that purely real eigenvalues $d_1(k)$ and $d_3(k)$ exist only for small wave numbers [inside the propagating gap for $z_1(k)$], while at some k value they merged. At this k point the two relaxing modes disappear, and the pair of propagating excitations $z_1^{\pm}(k)$ emerges instead. Only one relaxing mode $d_2(k)$ exists in the whole k region studied. The physical meaning of this mode will be discussed in more detail in Ref. [41].

From the behavior of eigenvalues at $k \rightarrow 0$ one can establish that the pair of propagating modes $z_2(k)$ corresponds to generalized sound excitations with linear dispersion $\omega_s(k)$ in the hydrodynamic region. For the reader’s convenience we have plotted the dispersions and damping coefficients of generalized sound excitations $z_2(k)$, obtained at different tem-

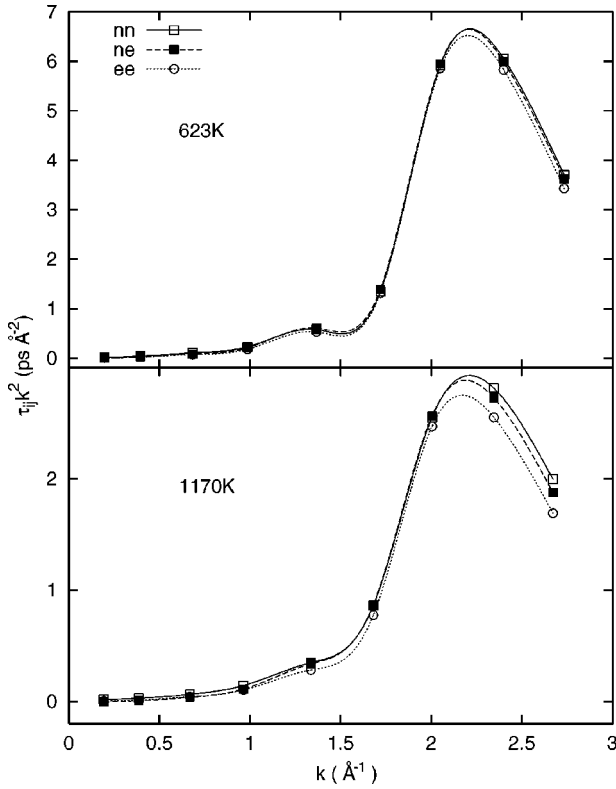


FIG. 5. Correlation times $\tau_{nn}(k)$ (open squares), $\tau_{ne}(k)$ (solid squares), and $\tau_{ee}(k)$ (open circles): all functions are calculated directly in MD simulations on the basis of Eq. (14) and multiplied by k^2 .

peratures, separately in Fig. 7. For small wave numbers the hydrodynamic behavior of the propagating sound excitations is well known [14,15] and is described by the expression

$$z_2^\pm(k) \approx \Gamma k^2 \pm i c_s k, \quad (19)$$

where c_s and Γ are the adiabatic sound velocity and sound attenuation coefficient, respectively. The straight dash-dotted lines in the upper frames of Figs. 6(a) and 6(b) allow one to see that the branch $z_2(k)$ has in both cases a small “positive dispersion,” which is in complete agreement with the predictions of mode coupling theory [35,36]. From the slope of the dash-dotted lines we are able to estimate the speed of longitudinal acoustic waves in liquid Pb. These values as well as the estimated values for the sound attenuation coefficients are given in Table I. We were able to find in the literature only an experimental value for the sound velocity of lead at the melting point, $c_s = 1790$ m/s [37], which is in quite nice agreement with our results given in Table I.

Beyond the hydrodynamic region the mode coupling effects become important and they change the hydrodynamic dependence (19). For intermediate values of k we can see in Fig. 7 that the real parts of the eigenvalues $z_2(k)$ behave almost like linear functions of k . Note that the departure from the hydrodynamic dependence (19) is on the side of lower values (negative dispersion), which is again in agreement with the predictions of the mode coupling theory [35,36]. It is worth mentioning that such a specific k dependence of the

dispersion and damping coefficients of the generalized sound mode just beyond the hydrodynamic region was associated in Ref. [11] with the crossover from viscous to elastic behavior. In the region of elastic behavior generalized sound excitations reflect some properties of so-called “zero-sound” excitations, known for solidlike systems. In order to clarify this problem additional study is needed.

Another interesting feature can be seen in Fig. 7 in the behavior of the dispersion curves $\text{Im} z_2(k)$ of generalized sound excitations at different temperatures. For the higher temperature $T_h = 1170$ K, the minimum of the dispersion curve at $k \approx k_p$ is much more pronounced than at $T_l = 623$ K. From real parts of the eigenvalues $z_2(k)$ one can conclude that at higher temperatures the damping of sound waves in the region of the maximum of $S(k)$ is much stronger. This implies that for very high temperatures one can expect the emergence of a propagating gap for sound excitations in this k region. We note also that for $T_h = 1170$ K in the region $k \approx k_p$ the negative amplitude, describing the mode contribution from the generalized sound excitations to the density-density time correlation function, has been obtained. This is in agreement with the result of Ref. [38]. We will report the study of mode contributions to the time correlation functions in Ref. [41].

In full agreement with standard hydrodynamics another generalized hydrodynamic eigenvalue, which is a purely real one in the small- k region and corresponds to the thermodiffusive mode, behaves like

$$d_1(k) \rightarrow D_T k^2, \quad k \rightarrow 0, \quad (20)$$

with D_T being the thermodiffusion coefficient. For the smallest k points we have estimated the values of D_T and the results are given in Table I. It should be noted that the smallest wave numbers reached in our MD for a liquid lead are not, in fact, in the hydrodynamic region, so that mode coupling effects could change the hydrodynamic dependences (19) and (20). Moreover, it is difficult to estimate the general tendency of the temperature dependence for the thermodiffusion coefficient and sound attenuation coefficient by considering just two thermodynamic points. This requires more detailed study and will be reported elsewhere.

The pair of propagating modes $z_2^\pm(k)$ together with the thermodiffusive mode $d_1(k)$ form the set of the generalized hydrodynamic collective excitations. All other eigenvalues correspond to kinetic modes, the damping coefficients of which, in contrast to generalized hydrodynamic ones, tend to some finite values when k goes to zero, so that these excitations have a finite lifetime and do not contribute to the hydrodynamic long-time behavior. However, as is seen in Fig. 6, the real parts of the generalized hydrodynamic and kinetic modes become comparable for intermediate and large values of k . Hence, the role of kinetic modes increases beyond the hydrodynamic region.

The spectra of generalized collective excitations, obtained within the nine-variable (11) treatment, contain in the small- k region two branches of kinetic propagating excitations and two kinetic relaxing modes. Note that the high-frequency branches of kinetic propagating modes $z_3^\pm(k)$ and $z_4^\pm(k)$ cor-

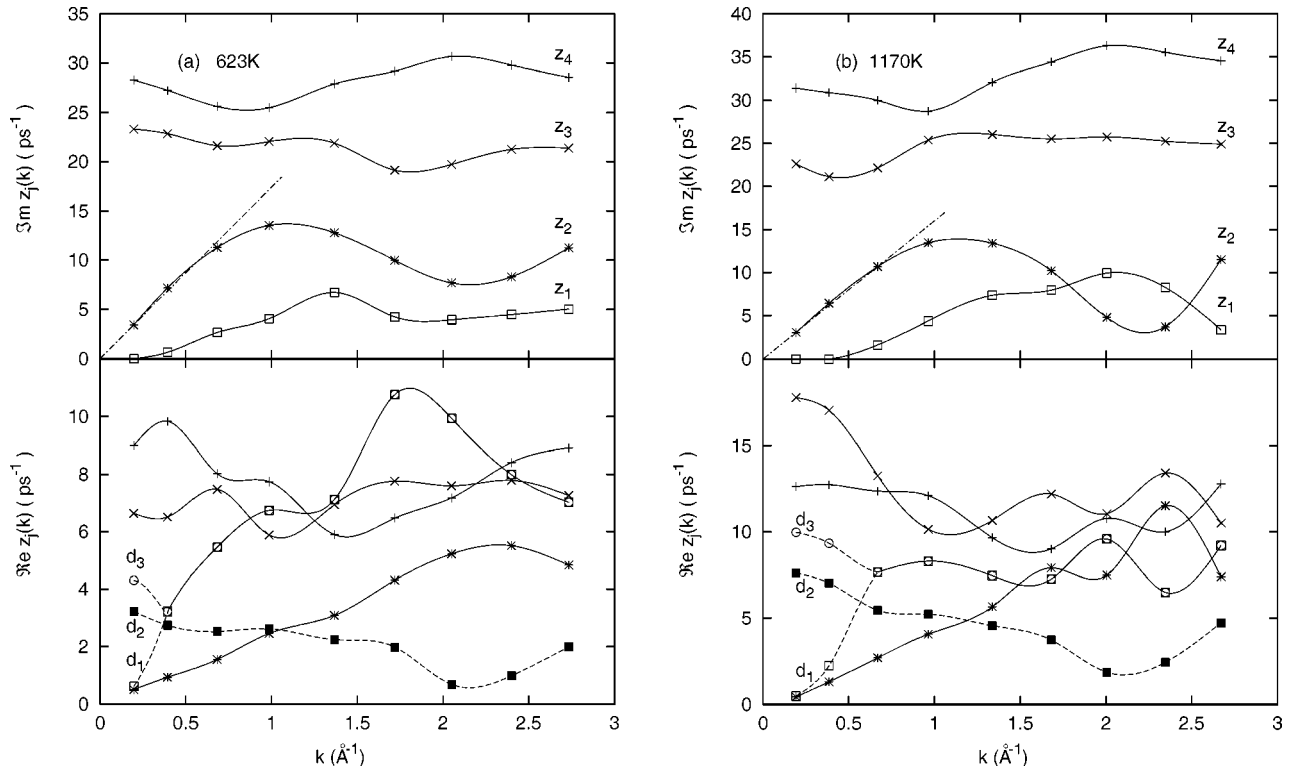


FIG. 6. Spectra of collective excitations of liquid Pb at 623 K (a) and 1170 K (b), obtained for the nine-variable basis set $\mathbf{A}^{(9)}(k,t)$. Complex and purely real eigenvalues are shown by symbols, connected by spline-interpolated solid and dashed lines, respectively. The same symbols in the upper and lower frames correspond to the imaginary and real parts of the propagating modes, except for the case of the splitting of the complex-conjugated eigenvalue $z_1(k)$ into two real ones for small k values. The straight dash-dotted lines in the upper frames show the linear hydrodynamic dispersion of sound excitations.

respond to extremely short-time excitations and appeared in our calculations because the dynamic variables with two and three dots in the basis set $\mathbf{A}^{(9)}(k,t)$ were taken into account [10,26]. When k increases, an additional branch $z_1^\pm(k)$ of propagating modes appears as a result of the coupling between the purely relaxing modes $d_1(k)$ and $d_3(k)$. In order to establish the physical meaning of these propagating excitations we have to perform a special analysis of spectrum formation. It is possible to do so by using separated subsets of the dynamical variables as was proposed, for instance, in [26].

D. Analysis of the physical origin of different branches of the propagating modes

To establish the origin of all kinetic branches in the spectrum of collective excitations in liquid lead, we have used the following quite general scheme. First, separated subsets of the dynamic variables, which have a clearer physical meaning, are introduced. For instance, one can split the basis set $\mathbf{A}^{(9)}(k,t)$ into two subsets of dynamic variables, describing the viscoelastic and thermal properties of a liquid, so that, on the second step of our analysis, the spectra of generalized collective modes are calculated for the separated subsets of dynamical variables. Third, the results obtained are compared with the spectrum found for the basis set $\mathbf{A}^{(9)}$. This allows us to investigate the origin of collective excitations and to estimate the role of mode coupling effects, caused by

the interplay between viscoelastic and thermal processes. For a weak coupling one can expect that some branches in the spectrum obtained for the ‘‘coupled’’ basis set $\mathbf{A}^{(9)}$ will be reproduced by branches evaluated on the separated subsets. Such a scheme was applied [9,26] to the study of the transverse dynamics in binary liquids and enabled us to prove the existence opticlike excitations in nonionic binary liquids and establish their origin.

Let us define a new dynamic variable $h(k,t)$ as follows:

$$h(k,t) = e(k,t) - \frac{f_{ne}(k)}{f_{nn}(k)} n(k,t). \quad (21)$$

It is easy to verify that this variable, in contrast to the energy density $e(k,t)$, is orthogonal [19,20] to the density of particles $n(k,t)$, so that the variable $h(k,t)$ is more convenient for an analysis of thermal properties, decoupled from the viscoelastic ones. Note that the set of the hydrodynamic variables $n(k,t), J(k,t), h(k,t)$ contains only orthogonal dynamic variables and can be extended by their time derivatives. The dynamical variable $h(k,t)$ describes, in fact, the heat density fluctuations [39,40], and in the hydrodynamic limit the thermodiffusive mode emerges exclusively due to heat density fluctuations. In Fig. 8 the MD results obtained at $T=1170$ K for the time correlation function $F_{hh}(k,t)$ are shown for different k values. One can see that even for the smallest value k_{\min} achieved in our MD simulations, this

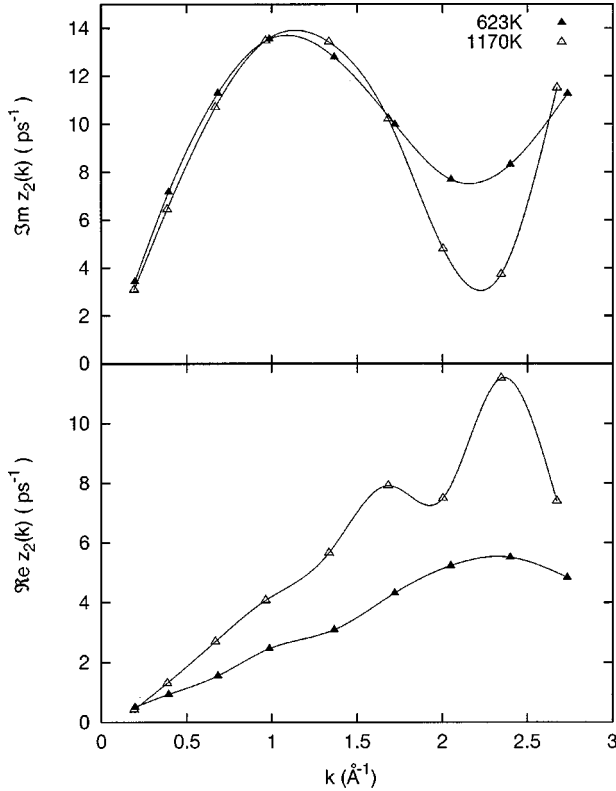


FIG. 7. Dispersion and damping coefficient of generalized sound excitations $z_2(k)$ for liquid Pb at 623 K (solid triangles) and 1170 K (open triangles). Solid lines denote the spline interpolation.

time correlation function does not have the single-exponential form expected from a separated treatment of heat fluctuations [39].

To understand the shape of time correlation functions $F_{hh}(k,t)$, shown in Fig. 6, we considered the “thermal” subset $\mathbf{A}^{(4h)}(k,t)$ of four dynamical variables,

$$\mathbf{A}^{(4h)}(k,t) = \{h(k,t), \dot{h}(k,t), \ddot{h}(k,t), \dddot{h}(k,t)\}, \quad (22)$$

which together with another separated subset $\mathbf{A}^{(5)}(k,t)$ (the “viscoelastic” one),

$$\mathbf{A}^{(5)}(k,t) = \{n(k,t), J_l(k,t), \dot{J}_l(k,t), \ddot{J}_l(k,t), \dddot{J}_l(k,t)\}, \quad (23)$$

form in fact the basis set $\mathbf{A}^9(k,t)$. Hence, one can expect that the spectra of generalized collective modes, obtained for the separated subsets (22) and (23), will reflect information

TABLE I. Estimated parameters of generalized hydrodynamic excitations for liquid Pb at two thermodynamic states: c_s , Γ , and D_T are the sound velocity, sound attenuation coefficient, and thermal diffusivity, respectively.

| T [K] | n [\AA^{-3}] | c_s [m/s] | Γ [10^{-7} m ² /s] | D_T [10^{-7} m ² /s] |
|---------|---------------------------|-------------|---|--------------------------------------|
| 623 | 0.030 94 | 1739.36 | 1.297 | 1.563 |
| 1170 | 0.028 90 | 1602.61 | 1.139 | 1.283 |

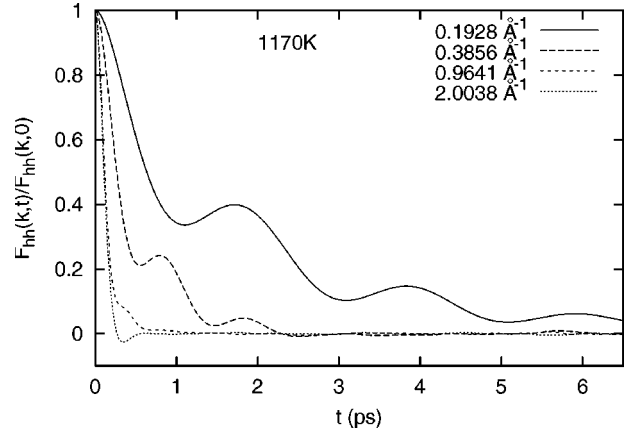


FIG. 8. Normalized “heat-density–heat-density” time correlation function $F_{hh}(k,t)$, obtained in MD simulations for four values of wave number k at the temperature $T_h=1170$ K.

about the decoupled thermal and viscoelastic properties of the system and will give us additional information about the origin of generalized collective modes, calculated for the “coupled” nine-variable set (11) (see Fig. 6). The results of our calculations, obtained for the separated subsets (22) and (23), are presented in Fig. 9 by dashed and solid spline-interpolated lines, respectively. For the sake of convenience, the dispersions of generalized collective modes, found for the “coupled” set (11), are also shown here by symbols. It is clearly seen that the propagating modes $z_1^\pm(k)$ are caused by

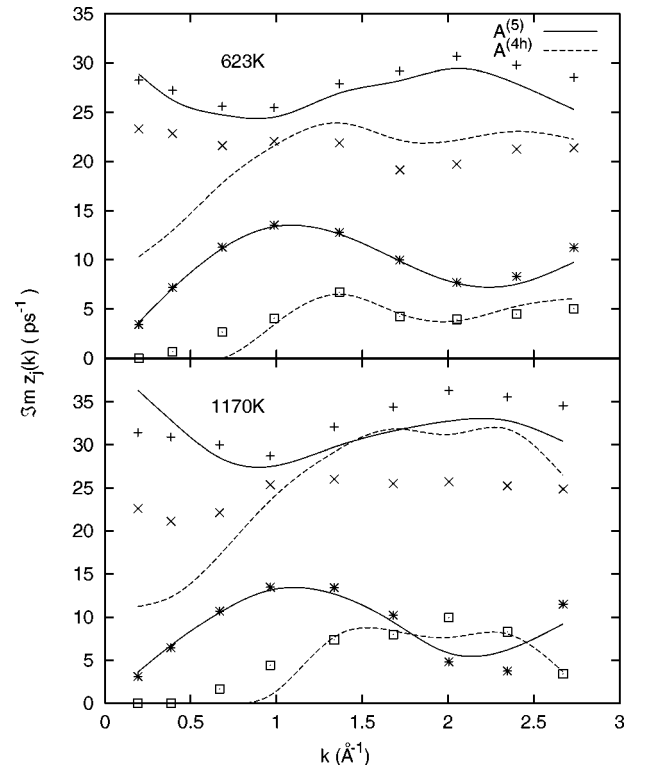


FIG. 9. Imaginary parts of propagating collective excitations, obtained for the separated subsets $\mathbf{A}^{(5)}(k,t)$ (spline interpolated, solid line) and $\mathbf{A}^{(4h)}(k,t)$ (spline interpolated, dashed line). Symbols denote the same eigenvalues as in Figs. 6(a) and 6(b).

heat fluctuations and describe the low-frequency heat waves. The branch $z_2^\pm(k)$ is well reproduced within the viscoelastic treatment and corresponds to generalized sound excitations. One can see also that in the region of the main peak location of the static structure factor $k \approx k_p$ the branch $z_2^\pm(k)$ has a minimum, which is much more pronounced at higher temperature. This implies that for very high temperatures one can expect in liquid Pb a propagation gap for generalized sound excitations with wave number $k \approx k_p$. The high-frequency branches $z_3^\pm(k)$ and $z_4^\pm(k)$ have mainly thermal and viscous origin, but their positions are strongly affected by lower branches due to the mode coupling effects. It is also interesting that for $k > 1 \text{ \AA}^{-1}$ the high-frequency branch of heat waves, obtained for the separated subset (22), follows qualitatively the shape of the low-frequency heat branch.

In our recent studies of the dynamical properties for liquid Bi [23] and Cs [34], performed within the nine-variable GCM approach, the high-frequency branches of heat waves have been obtained with the k dependence being very similar to one found for the high-frequency heat modes in liquid lead (see symbols and upper dashed lines in Fig. 9). In contrast to the case of liquid Pb, where the propagation gap for the low-frequency heat waves is found to be very small, $k_H \approx 0.4 \text{ \AA}^{-1}$, the propagating gap in liquid Cs was much wider ($k_H \approx 2 \text{ \AA}^{-1}$), and for liquid semimetallic Bi the low-frequency branch of heat waves was not found at all within the range of k studied ($k < 3 \text{ \AA}^{-1}$). Comparing the behavior of two branches of heat waves, obtained for the separated subset $\mathbf{A}^{(4h)}(k, t)$ (upper dashed lines in Fig. 9) and within the nine-variable treatment (shown by symbols in Fig. 9), one can make the following conclusion: the dynamical coupling between heat and viscous processes leads to a reduction of the propagation gap for low-frequency heat waves and pushes upwards the high-frequency branch of heat waves in the range of small and intermediate values of wave numbers.

E. Low-frequency heat waves: Condition of existence

In order to understand the difference found for the low-frequency heat waves in liquid Pb and liquid Cs and to obtain the expression for the propagating gap, which allows us to estimate roughly its width, an additional investigation has to be performed. It could be done by taking into account that the coupling between heat and density fluctuations becomes negligible when the ratio (18) of generalized specific heats $\gamma(k)$ is close to 1.0 [14,15]. Having this in mind let us consider the simplest nontrivial approximation within the GCM approach which follows from a two-variable description, based only on the heat density operators. Note that in the one-variable approximation an one-exponential form [39]

$$F_{hh}^{(1)}(k, t)/F_{hh}^{(1)}(k, 0) = e^{(-\lambda/nC_V)k^2 t} \quad (24)$$

for the time correlation function $F_{hh}^{(1)}(k, t)$ follows immediately from our scheme, where λ and n are the thermal conductivity coefficient and the number density, respectively. In Fig. 8 one can see that even for $k \approx k_{\min}$ the MD-derived function $F_{hh}(k, t)$ contains oscillations, which appear due to

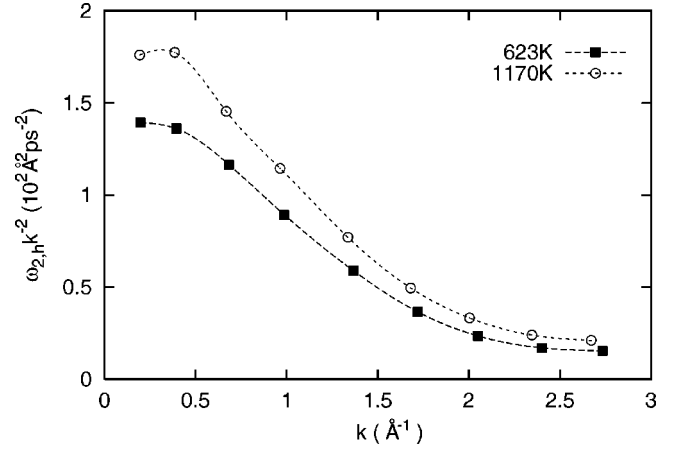


FIG. 10. The second frequency moment of the “heat-density–heat-density” time correlation function, divided by k^2 , at temperatures $T_l = 623 \text{ K}$ (squares) and $T_h = 1170 \text{ K}$ (circles).

contributions of acousticlike excitations. However, as can be proved analytically within the hydrodynamic approach, this function is well described for small wave numbers by an exponential function (24) with weak acoustic oscillations of order of magnitude $\sim (1 - 1/\gamma)$. Thus, in the case of liquid metals, when γ is close to unity, the approximated expression (24) for the treatment of heat fluctuations could be considered as acceptable.

Within a two-variable approximation, which was previously used by us for the description of shear waves in liquids [20,22,10], one can write down the expression for the generalized hydrodynamic matrix (4), evaluated for the two-variable set $\mathbf{A}^{(2h)} = \{h(k, t), \dot{h}(k, t)\}$, as follows:

$$\mathbf{T}(k) = \mathbf{F}^0(k, 0) [\tilde{\mathbf{F}}^0(k, 0)]^{-1} = \begin{pmatrix} 0 & -1 \\ \bar{\omega}_{2,h} & \bar{\omega}_{2,h} \tau_h \end{pmatrix}, \quad (25)$$

where the k -dependent Maxwell-like time of relaxation $\tau_h(k)$ is defined by Eq. (14), and the function $\bar{\omega}_{2,h}(k)$ is the second-order frequency moment of $F_{hh}(k, t)$, namely, $\bar{\omega}_{2,h}(k) = f_{\dot{h}\dot{h}}(k)/f_{hh}(k)$. In Fig. 10 one can see that the function $\bar{\omega}_{2,h}(k)$ in the small- k region is proportional to k^2 . Taking into account the definition (21) and the conserved properties of the hydrodynamic variables $e(k, t)$ and $n(k, t)$, such a behavior can be obtained analytically. This allows us to rewrite the second-order frequency moment $\bar{\omega}_{2,h}(k)$ as follows:

$$\bar{\omega}_{2,h}(k) = \frac{k^2 G^h(k)}{\rho}, \quad (26)$$

where ρ is the mass density and we introduced the function $G^h(k)$ with the dimensionality of pressure, which has an analogy with the rigidity modulus in the case of transverse dynamics. In the case of heat fluctuations $G^h(k)$ can be called as a k -dependent heat-rigidity modulus. Obviously, $G^h(k)$ tends to a constant in hydrodynamic limit. The formal analogy in the treatment between the heat and shear pro-

cesses is well known in the theory of continuous media [12]. Let us use this analogy to get an interpretation for our theoretical results obtained in the framework of statistical physics.

Using Eq. (25) one can immediately write down the expression for the eigenvalues of the generalized hydrodynamic matrix $\mathbf{T}(k)$ in the two-variable approximation:

$$z_h^\pm(k) = \frac{\bar{\omega}_{2,h}(k)\tau_h(k)}{2} \pm \left[\frac{\bar{\omega}_{2,h}^2(k)\tau_h^2(k)}{4} - \bar{\omega}_{2,h}(k) \right]^{1/2}. \quad (27)$$

This equation gives in fact the spectrum of heat excitations in our simplified theory. One can see that there exists two different kinds of solutions (27). In the case when

$$\frac{\bar{\omega}_{2,h}\tau_h^2(k)}{4} < 1, \quad (28)$$

one has two complex-conjugated eigenvalues

$$z_h^\pm = \sigma_h(k) \pm i\omega_h(k),$$

which describe the heat waves, propagating in opposite directions, with frequency $\omega_h(k)$ and damping $\sigma_h(k)$. Otherwise, we find two purely relaxing modes as was observed in Fig. 6.

The condition (28) allows us to estimate the width of the propagating gap in which the low-frequency heat waves are not supported by a liquid. For a rough estimation the expression (24) can be used for the calculation of the correlation time $\tau_h(k)$. Then, using Eq. (26) for small values of k , we get the following equation:

$$k_H \approx \frac{nC_V}{2\lambda} \sqrt{\frac{G^h}{\rho}}, \quad (29)$$

so that for $k < k_H$ (inside the propagation gap) one has two purely real eigenvalues, which in the small- k region behave like

$$z_h^+(k) = d_{2h}(k) = \frac{C_V G^h}{m\lambda} - \frac{\lambda}{nC_V} k^2,$$

$$z_h^-(k) = d_{1h}(k) = \frac{\lambda}{nC_V} k^2.$$

Note that the eigenvalue $z_h^-(k)$ describes just the thermodiffusive hydrodynamic mode, calculated in the viscoelastic approximation (see [39]). Beyond the propagating gap ($k < k_H$) we find two propagating excitations with complex-

conjugated eigenvalues. It is worth mentioning that Eq. (29) can be improved if we use for the calculation of $\tau_h(k)$ a more precise expression for the time correlation function $F_{hh}(k,t)$, which is known from hydrodynamic three-variable theory [14,15]. In such a case viscoelastic effects could be partly taken into consideration. However, the general picture will remain the same: there always exists a propagation gap for the low-frequency heat waves in a liquid with the width depending on the values of the thermal conductivity, specific heat at constant volume, and heat-rigidity modulus.

We end this section with an expression for the time correlation function $F_{hh}(k,t)$ found in the two-variable approximation:

$$\begin{aligned} \frac{F_{hh}^{(2)}(k,t)}{F_{hh}^{(2)}(k,0)} = & - \frac{z_h^-(k)}{z_h^+(k) - z_h^-(k)} e^{-z_h^+(k)t} \\ & + \frac{z_h^+(k)}{z_h^+(k) - z_h^-(k)} e^{-z_h^-(k)t}. \end{aligned} \quad (30)$$

It is important to note that this expression reproduces explicitly the frequency moments of the genuine function $F_{hh}(k,t)$ up to the second order included.

IV. CONCLUSIONS

The main results of this study are the following.

(i) Beyond the hydrodynamic region the spectrum of collective excitations of liquid metallic Pb, obtained within the nine-variable approximation of the parameter-free method of generalized collective modes, contains four branches of propagating excitations: generalized sound modes and one low- and two high-frequency branches of *kinetic* modes.

(ii) Heat fluctuations cause not only thermodiffusive processes, but for larger wave numbers they also stimulate the appearance of two branches of heat waves. In liquid lead there exists a rather small propagation gap for the low-frequency heat waves.

(iii) A simple analytical two-variable treatment allows one to explain the existence of the propagation gap for low-frequency heat waves and to estimate its width.

In Ref. [41] we will report the results obtained for the mode contributions to time correlation functions and focus more attention on the role of the purely relaxing kinetic mode $d_2(k)$.

ACKNOWLEDGMENT

I.M. thanks the Fonds für Förderung der wissenschaftlichen Forschung under Project No. P12422 TPH for support.

[1] N. H. March, *Liquid Metals: Concepts and Theory* (Cambridge University Press, Cambridge, England, 1990).
 [2] M. Dzugutov and U. Dahlborg, *Phys. Rev. A* **40**, 4103 (1989).
 [3] F. J. Bermejo, R. Fernandez-Perea, M. Alvarez, B. Roessli, H. E. Fischer, and J. Bossy, *Phys. Rev. E* **56**, 3358 (1997).

[4] J. Bosse, G. Jacucci, M. Ronchetti, and W. Schirmacher, *Phys. Rev. Lett.* **57**, 3277 (1986).
 [5] A. Campa and E. G. D. Cohen, *Phys. Rev. Lett.* **61**, 853 (1988).
 [6] M. Alvarez, F. J. Bermejo, P. Verkerk, and B. Roessli, *Phys.*

- Rev. Lett. **80**, 2141 (1998).
- [7] M. Parrinello and M. P. Tosi, Riv. Nuovo Cimento **2**, 1 (1979).
- [8] N. H. March and M. Parrinello, *Collective Effects in Solids and Liquids* (Hilger, Bristol, 1982).
- [9] T. Bryk and I. Mryglod, Phys. Lett. A **261**, 285 (1999).
- [10] T. Bryk and I. Mryglod, J. Phys.: Condens. Matter **12**, 6063 (2000).
- [11] Chr. Morkel, T. Bodensteiner, and H. Gemperlein, Phys. Rev. E **47**, 2575 (1993).
- [12] D. D. Joseph and L. Preziosi, Rev. Mod. Phys. **61**, 41 (1989).
- [13] I. M. Mryglod and I. P. Omelyan, Phys. Lett. A **205**, 401 (1995).
- [14] J.-P. Boon and S. Yip, *Molecular Hydrodynamics* (New York, McGraw-Hill, 1980).
- [15] J.-P. Hansen and I. R. McDonald, *Theory of Simple Liquids* (Academic, London, 1986).
- [16] R. L. McGreevy and E. W. J. Mitchell, Phys. Rev. Lett. **55**, 398 (1985).
- [17] C. Bruin, J. P. J. Michels, J. C. van Rijs, L. A. de Graaf, and I. M. de Schepper, Phys. Lett. A **110**, 40 (1988).
- [18] I. M. de Schepper, E. G. D. Cohen, C. Bruin, J. C. van Rijs, W. Montfrooij, and L. A. de Graaf, Phys. Rev. A **38**, 271 (1988).
- [19] I. M. Mryglod, I. P. Omelyan, and M. V. Tokarchuk, Mol. Phys. **84**, 235 (1995).
- [20] I. M. Mryglod, Condens. Matter Phys. (Ukraine) **1**, 753 (1998).
- [21] T. Bryk and Y. Chushak, J. Phys.: Condens. Matter **9**, 3329 (1997).
- [22] T. Bryk and I. Mryglod, J. Phys. Stud. (Ukraine) **2**, 322 (1998).
- [23] T. Bryk and I. Mryglod, J. Phys.: Condens. Matter **12**, 3543 (2000).
- [24] D. Bertolini and A. Tani, Phys. Rev. E **51**, 1091 (1995).
- [25] Note that in the case of binary liquids already within the hydrodynamic treatment one has to include in addition (comparing with a simple fluid) the dynamic variable, which describes the mass-concentration fluctuations. This results in a higher number N_v of dynamical variables to be considered within the GCM approach. For details we refer the reader to recent GCM studies of dynamical properties in binary mixtures [10,26,28].
- [26] T. Bryk and I. Mryglod, Phys. Rev. E **62**, 2188 (2000).
- [27] P. Westerhuijs, W. Montfrooij, L. A. de Graaf, and I. M. de Schepper, Phys. Rev. A **45**, 3749 (1992).
- [28] T. Bryk, I. Mryglod, and G. Kahl, Phys. Rev. E **56**, 2903 (1997).
- [29] T. Bryk and I. Mryglod, Condens. Matter Phys. (Ukraine) **2**, 285 (1999).
- [30] The “parameter-free form” is a term which means that all calculations needed can be performed in the GCM approach without any adjustable parameters. As theory input one has to take the pair interaction potential, the density of particles $n = N/V$, and temperature T . Then, combining MD simulations for the static correlation functions and the “hydrodynamic” correlation times with the analytical expressions derived, one can calculate the spectrum of collective excitations and the mode contributions to time correlation functions as well as the generalized transport coefficients [20]. In its original formulation [18,27] this method contained several adjustable parameters, which had to be estimated from the fitting procedure to MD-derived time correlation functions or to the experimental values of transport coefficients [18,27].
- [31] I. M. Mryglod and I. P. Omelyan, Mol. Phys. **91**, 1005 (1997).
- [32] I. Mryglod, Ukr. Phys. J. **43**, 252 (1998).
- [33] M. Dzugutov, in *Static and Dynamic Properties of Liquids*, edited by M. Davidovic and A. K. Soper (Springer-Verlag, Berlin, 1989).
- [34] T. Bryk and I. Mryglod (unpublished).
- [35] I. M. de Schepper, P. Verkerk, A. A. van Well, and L. A. de Graaf, Phys. Lett. A **104**, 29 (1984).
- [36] I. Mryglod, J. Phys. Stud. (Ukraine) **3**, 33 (1999).
- [37] I. Dubrovskii, B. Yegorov, and K. Ryaboshapka, *Handbook of Physics* (Naukova Dumka, Kiev, 1986).
- [38] I. M. de Schepper, P. Verkerk, A. A. van Well, and L. A. de Graaf, Phys. Rev. Lett. **50**, 974 (1983).
- [39] N. H. March and M. P. Tosi, *Atomic Dynamics in Liquids* (Macmillan, London, 1976).
- [40] U. Balucani and M. Zoppi, *Dynamics of the Liquid State* (Clarendon, Oxford, 1994).
- [41] T. Bryk and I. Mryglod, Phys. Rev. E (to be published).